

# Polarized luminescence from self-assembled, aligned, and cleaved supramolecules of highly ordered rodlike polymers

M. Knaapila and O. Ikkala<sup>a)</sup>

*Department of Engineering Physics, Helsinki University of Technology, Espoo, Finland*

M. Torkkeli, K. Jokela, and R. Serimaa

*Department of Physical Sciences, University of Helsinki, Helsinki, Finland*

I. P. Dolbnya and W. Bras

*Netherlands Organization for Scientific Research (NWO) DUBBLE CRG/ESRF, Grenoble, France*

G. ten Brinke

*Materials Science Center, University of Groningen, Groningen, The Netherlands*

L. E. Horsburgh, L.-O. Pålsson, and A. P. Monkman<sup>b)</sup>

*Department of Physics, University of Durham, Durham, United Kingdom*

(Received 21 February 2002; accepted for publication 14 June 2002)

A hierarchical self-assembly in comb-shaped supramolecules of conjugated rodlike polymers is reported. The supramolecules consist of poly(2,5-pyridinediyl), acid dopants, and hydrogen bonded alkyl side chains. A thermotropic smectic state with an exceptionally large coherence length is formed without additional solvent. This allows facile overall alignment resulting in high dichroism and polarized photoluminescence. Solid films are formed by cleaving side groups from the supramolecules which retain the optical anisotropy together with the high photoluminescence quantum yield of pristine polymer. © 2002 American Institute of Physics.

[DOI: 10.1063/1.1499222]

Manipulation of electro-optical properties in conjugated materials requires control of molecular packing and overall order. Single crystals of oligomers<sup>1</sup> provide spectacular electronic properties but may demand nontrivial deposition techniques. Self-organization in solution-processed polymers, particularly in poly(alkylthiophene)s (PAT)s,<sup>2–5</sup> also yields highly developed local order with feasible electronic characteristics.<sup>4</sup> However, a high overall order is difficult to obtain due to coiling, a problem that could be overcome with rodlike polymers.

Polypyridines are stable polymers with good electronic properties. Poly(2,5-pyridinediyl) (PPY), is among the simplest rodlike polymers; yet, it contains specific sites needed to construct supramolecules. Their design<sup>6</sup> is difficult due to aggregation, limited solubility, and the demand for chemical stability in acidic solvents. In this work, comb-shaped supramolecules of PPY have been developed based on protonation of pyridine moieties by camphorsulfonic acid (CSA) and hydrogen bonding alkylresorcinol or gallate side groups, which contain the repulsive alkyl chains required for mesomorphism.<sup>7</sup> Partial CSA complexation leads to efficient photoluminescence (PL) as the pyridyl nitrogen lone pair is orthogonal and unconjugated with the ring  $\pi$  cloud.<sup>8</sup> The side groups can also be regarded as hydrogen bonding solvents allowing high solubility, due to matching hydrogen bonds. This concept allows phase tailoring all the way from crystals to disordered liquid. This is uncommon, as a liquid crystalline (LC) state is difficult to achieve using general solvents, such as formic acid. The crucial difference between the chemically and physically bonded side chains is that the

latter can be removed, i.e., cleaved by a vacuum under heating. When this is done after alignment in the LC state, the resultant solid material retains high structural anisotropy yielding polarized PL with relatively high PL quantum yield (PLQY) (Fig. 1). By removing the bulky side groups, close interchain packing can be achieved with oriented chains, suppressing cross over points which would be potential sites of aggregation or excimer formation.

PPY was complexed by CSA to form  $\text{PPY}(\text{CSA})_x$ . Amphiphilic molecules 5-pentyl-1,3-dihydroxybenzene (PRES), 4-hexyl-1,3-dihydroxybenzene (HRES), octyl phenol (OP), or 1-octyl-3,4,5-trihydroxybenzoate (OG) were hydrogen bonded to  $\text{PPY}(\text{CSA})_x$ .<sup>7,9</sup> The resulting complexes are denoted as  $\text{PPY}(\text{CSA})_x(\text{amphiphile})_y$ . To prevent macrophase separation only selected  $x, y$  values are allowed. Complexes were studied using x-ray diffraction<sup>7,9</sup> and photophysical<sup>8,10</sup> techniques.

The starting materials are crystalline.  $\text{PPY}(\text{CSA})_x$  is an infusible solid. In the following, not all pyridine groups have been protonated, i.e.,  $x < 1$ , as this maintains strong PL.<sup>8</sup> When the amphiphiles are introduced, for small  $x$  and  $y$ , e.g.,  $x = 0.25, y = 0.25$ , or 0.5, a glassy birefringent material between 25 °C–200 °C is obtained. For increased values,  $x = y = 0.5$ , a glassy material is observed at 25 °C but at mod-

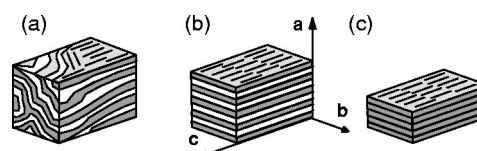


FIG. 1. (a) Self-assembled local structure. White layers denote side chains. (b) Alignment leads to macroscopically ordered structure characterized by axes **a**, **b**, and **c**. (c) Solid films due to cleavage of the side chains.

<sup>a)</sup>Electronic mail: olli.ikkala@hut.fi

<sup>b)</sup>Electronic mail: a.p.monkman@durham.ac.uk

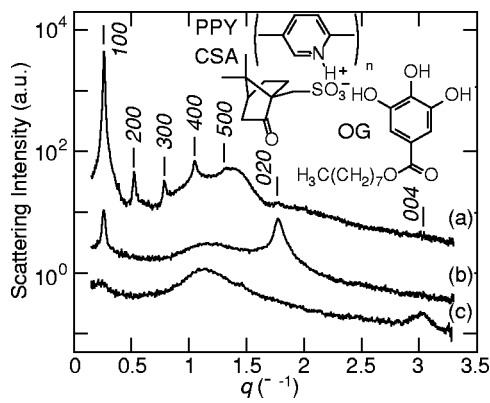


FIG. 2. X-ray diffraction curves of aligned PPY(CSA)<sub>0.5</sub>(OG)<sub>0.5</sub> in three directions: (a) Normal i.e., equatorial out-of-plane, a. (b) Equatorial, i.e., equatorial in-plane, b. (c) Meridional, c.

erate temperatures, a birefringent fluid is formed with a broad endothermic differential scanning calorimetry rise, typical for noncrystalline materials. X-ray diffraction curves show several sharp reflections following the sequence  $q^*$ ,  $2q^*$ ,  $3q^*$ , ..., which indicates a lamellar structure.<sup>7</sup> At higher  $q$  values, there is a broad amorphous halo at  $\sim 1\text{--}1.5 \text{ \AA}^{-1}$  arising from inter- and intrachain short-range order. A sharp reflection is superimposed on the amorphous halo near  $1.8 \text{ \AA}^{-1}$  and, depending on the composition, an additional reflection is also observed at  $3.0\text{--}3.2 \text{ \AA}^{-1}$ . A further increase of  $x$  and  $y$  results in a LC state even at  $25 \text{ }^\circ\text{C}$  and a transition to an isotropic (nonbirefringent) disordered fluid at a higher temperature. If  $y/x \geq 2$ , a biphasic system is usually seen.

Solution cast films ( $\sim 10 \text{ }\mu\text{m}$ ) were sheared in the *in-plane* direction by drawing them along the substrate surface. In particular, no rubbed substrates were used. Rigid polymers are expected to align with their chain axes in the drawing direction and the lamellae parallel to the surface. X-ray diffraction patterns were measured *ex situ* in three directions with respect to the aligned sample, see Fig. 2.

The structure is orthorhombic with axes **a**, **b**, and **c** [Fig. 1(b)]. The reflections from the lamellar structure are in the *equatorial out-of-plane* direction, **a**, and are denoted as  $h00$ . The interlayer distance  $d_{100} \cong 2\pi/q^*$  is dependent on the side-chain length, as expected, but does not follow the simple scheme of side-chain tilt and interdigitation.

The reflection near  $1.8 \text{ \AA}^{-1}$  is in the *equatorial in-plane*, **b**, and is assigned as  $020$ . The pyridine rings stack perpendicular to the surface and the corresponding Bragg spacing ( $3.55 \text{ \AA}$ ) describes the stacking distance being nearly the same as in the pure PPY. The position of reflection  $020$  is independent of the side-chain length but disappears on increasing the side group concentration ( $x, y$ ) and/or the temperature. It is absent in the corresponding complexes of *meta*-coupled (kinked) poly(2,6-pyridinediyl) or flexible poly(4-vinylpyridine) which do not form well-defined structures in the main chain direction due to coiling. In bulk samples ( $\sim 1 \text{ mm}$ ), the  $020$  reflections are asymmetric, because they include reflections  $120$ ,  $220$ , etc., which are not resolved due to the limited crystallite size.

The reflection at  $3.0\text{--}3.1 \text{ \AA}^{-1}$  is in the meridional direction, **c**, and may be assigned as  $004$  since the Bragg distance ( $\sim 2.1 \text{ \AA}$ ) corresponds to one fourth of the length of the suggested PPY(CSA)<sub>0.5</sub> repeat unit. In pure PPY, the peak is at

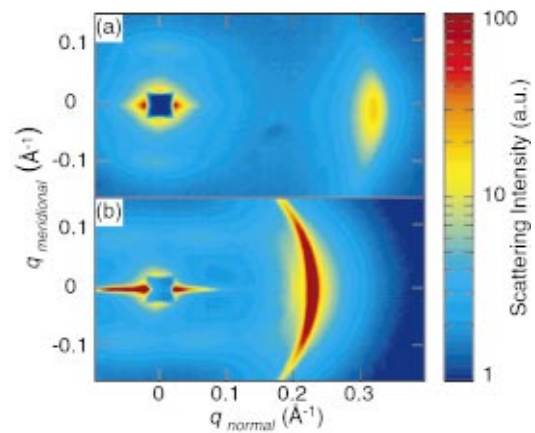


FIG. 3. (Color) Two-dimensional x-ray diffraction patterns at low angle. (a) Solid PPY(CSA)<sub>0.25</sub>(PRES)<sub>0.25</sub>. (b) Fluid PPY(CSA)<sub>0.5</sub>(OP)<sub>1.0</sub> at  $25 \text{ }^\circ\text{C}$ .

$3.11 \text{ \AA}^{-1}$ , having an asymmetric form. The reflection at  $3.1 \text{ \AA}^{-1}$  is related to the intrachain distance of the pyridine groups.

Prominent reflections at  $\sim 0.09 \text{ \AA}^{-1}$  are also seen along the meridional direction for the hard solid samples, e.g.,  $x, y \leq 0.25$  [Fig. 3(a)]. Their appearance is concomitant to broadening of the  $100$  reflections in samples with low side group concentration. In the fluidlike PPY(CSA)<sub>0.5</sub>(OP)<sub>1.0</sub> these reflections also appear but as parallel streaks akin to nematic liquid systems of rodlike molecules [Fig. 3(b)]. As all these features are observed, a third level of organization, i.e., supramolecular hierarchy, unique in conjugated polymers, must be present. Monodisperse rodlike polymers<sup>11</sup> or oligomers<sup>12</sup> can form superstructures where the chain ends are distributed in planes whose spacing corresponds to end-to-end distance of the chains. Here, the spacing ( $70 \text{ \AA}$ ) is commensurate with the length of PPY.

Grazing-incidence x-ray diffraction reveals the same structural features in spin-coated films ( $< 100 \text{ nm}$ ). The layers align parallel to the quartz surface and the  $h00$  maxima are found in the *out-of-plane* direction.<sup>9</sup> Sharp reflections  $020$  and  $004$  are in the *in-plane* direction. This resembles regioregular poly(3-hexylthiophene) (P3HT).<sup>4</sup> No self-organization promotor is needed here, unlike P3HT.

The layers are free floating under pressure. This implies freedom of motion for the polymer chains stacked in the lamellae explaining the absence of the nonaxial  $hk0$  reflections which should be present in a true crystal. Both  $h00$  and  $020$  reflections show well-defined arcs suggesting two-dimensional order in the  $(hk0)$  plane in the range of at least  $100 \text{ \AA}$ . To account for the mesomorphism and the absence of  $hk0$  peaks, both the layers and the stacks are assumed to undulate as in the paracrystalline model. The nonregioregularity of PPY and the racemicity of CSA may further suppress the crystallinity and favor the mesomorphism.

Correlation functions indicate highly ordered packing of lamellae and/or a narrow lamellar distribution (Fig. 4) with unusually large coherence lengths (Table I). The peak width of the higher-order reflections  $h00$  depend nearly linearly on  $q$ . Therefore, the reflection widths are predominantly due to lattice parameter fluctuations (microstrains) and the actual crystallite size may be considered far larger. The order be-

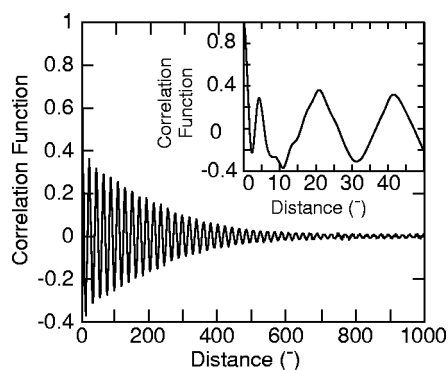


FIG. 4. The normalized  $\gamma(0)=1$  correlation function  $\gamma(r) = \int q^{-2} I(q) \cos(qr) dq$  normal to lamellae of PPY(CSA)<sub>0.5</sub>(HRES)<sub>0.5</sub> using  $q$  range between 0–2.2 Å<sup>-1</sup>. The maximum at 21 Å corresponds to  $d_{100}$  and the peak at 4 Å corresponds to the flat halo between 1–1.5 Å<sup>-1</sup> related to internal structure along the  $a$  axis.  $\alpha=\beta=\gamma=90^\circ$ ,  $a=20.06$  Å,  $b=6.89$  Å, and  $c=8.40$  Å.

tween layers is better than that of PATs, such as P3HT<sup>5</sup> or poly(3-dodecylthiophene) (P3DT),<sup>3</sup> or rigid monodisperse oligomers.<sup>12</sup> The structure can also be permanently improved by annealing, possibly due to release of strain and increase in the size of ordered domains. Such effects are reversible in P3DT,<sup>2</sup> for example.

Figure 5 shows the *in-plane* photoabsorption (PA) and PL emission of the aligned films. Strong PA is observed if the  $c$  axis is parallel to the polarization of the light. The two PA spectra have a slightly different shape and the parallel PA profile has also a slightly redshifted maximum relative to the perpendicular case. This has also been observed in stretch oriented PPY films<sup>10</sup> and is ascribed to a larger delocalization length in the ordered chains. The PL spectra depend strongly on the polarization of the excitation and the emitted light, leading to a five-fold difference in intensity between the parallel and perpendicular case. In contrast to the PA spectra, the two PL spectra have similar shapes. This suggests that the origin of PL is the same in both cases and indicates exciton migration to chain sites of lowest energy. Both PA and PL suggest that the major transition dipoles are oriented parallel to the  $c$  axis as is typical for this class of polymers. The PLQY is of the order of few %.

The side groups were cleaved in a vacuum (Fig. 1). The films remain optically anisotropic as revealed by polarized PL, i.e., the alignment of the polymer chains is not lost upon cleavage. For example, after heating the cast film of PPY(CSA)<sub>0.5</sub>(HRES)<sub>0.5</sub> at 120 °C for 42 h ( $\sim 10^{-3}$  mbar), Fourier-transform infrared spectrum reminiscent of PPY(CSA)<sub>0.5</sub> is seen, suggesting removal of HRES

TABLE I. Long period  $d_{100}$ , full width at half maximum (FWHM) of reflection 100, and coherence length normal to lamellae  $L \cong \lambda / (\Delta 2\theta \cos \theta)$  ( $2\theta$ =scattering angle). Instrumental function was taken into account by means of beam divergence and spatial resolution of the detector.

Complex	$d_{100}$ (Å)	FWHM (Å <sup>-1</sup> )	$L$ (Å)
PPY(CSA) <sub>0.5</sub> (OG) <sub>0.5</sub>	24	0.0073	790
PPY(CSA) <sub>0.5</sub> (OP) <sub>1.0</sub>	27	0.0077	750
PPY(CSA) <sub>0.5</sub> (HRES) <sub>0.5</sub>	21	0.0085	670
PPY(CSA) <sub>0.5</sub> (PRES) <sub>0.5</sub>	20	0.0076	760

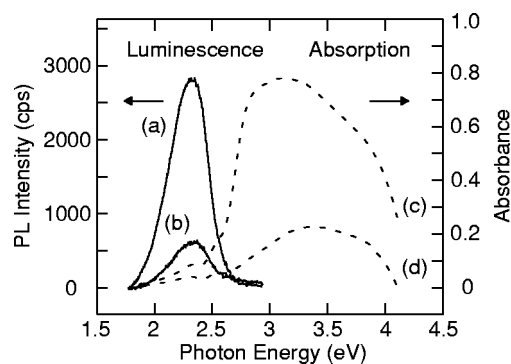


FIG. 5. The PL spectra of aligned films of PPY(CSA)<sub>0.5</sub>(HRES)<sub>0.5</sub> (solid lines) obtained with the  $c$  axis in vertical orientation: Both the excitation light ( $\lambda=370$  nm) and the PL are polarized (a) parallel and (b) perpendicular to the  $c$  axis. The PA curves (dashed lines) measured with polarized light. (c) The  $c$  axis parallel to the polarization vector of the probe light. (d) Their mutual perpendicular orientation.

( $T_m=68$  °C). Corresponding spin-coated films reveal x-ray diffraction patterns like PPY and PLQY increases from ( $10 \pm 1$ )% to ( $20 \pm 1$ )%, i.e. the same as PPY(CSA)<sub>0.5</sub> and PPY. A similar result is seen for PRES ( $T_m=48$  °C), whereas OG ( $T_m=102$  °C) shows signs of residual. Nevertheless, for the cast films of PPY(CSA)<sub>0.5</sub>(OG)<sub>0.5</sub> kept at 120 °C for 72 h *in vacuo*, the PLQY increased from  $\sim 1\%$  to ( $7 \pm 1$ )%. Hence, the actual mechanism of the PLQY increase may be the result of structural improvements and cleavage combined. PPY does not undergo thermal degradation.

Starting from the conjugated rodlike polymer, PPY, well-controlled micro- and macrostructures can be formed. Self-assembly is accomplished by supramolecules using amphiphiles which are hydrogen bonded to protonated PPY. Such a system forms hierarchically ordered structures, which have not hitherto been reported in conjugated polymers. Alignment of the polymers results in optical anisotropy, which is retained after cleavage of the alkyl chains.

The authors thank the Academy of Finland and the Finnish Cultural Foundation.

<sup>1</sup>J. H. Schön, Ch. Kloc, and B. Batlogg, *Science* **288**, 2338 (2000).

<sup>2</sup>K. Tashiro, K. Ono, Y. Minagawa, M. Kobayashi, T. Kawai, and K. Yoshino, *J. Polym. Sci., Part B: Polym. Phys.* **29**, 1223 (1991).

<sup>3</sup>T. J. Prosa, J. Moulton, A. J. Heeger, and M. J. Winokur, *Macromolecules* **32**, 4000 (1999).

<sup>4</sup>H. Siringhaus, P. J. Brown, R. H. Friend, M. M. Nielsen, K. Bechgaard, B. M. W. Langeveld-Voss, A. J. H. Spiering, R. A. J. Janssen, E. W. Meijer, P. Herwig, and D. M. de Leeuw, *Nature (London)* **401**, 685 (1999).

<sup>5</sup>K. E. Aasmundtveit, E. J. Samuelsen, M. Guldstein, C. Steinsland, O. Flornes, C. Fagermo, T. M. Seeberg, L. A. A. Pettersson, O. Inganäs, R. Feidenhans'l, and S. Ferrer, *Macromolecules* **33**, 3120 (2000).

<sup>6</sup>S. S. Zhu, P. J. Carroll, and T. M. Swager, *J. Am. Chem. Soc.* **118**, 8713 (1996).

<sup>7</sup>M. Knaapila, J. Ruokolainen, M. Torkkeli, R. Serimaa, L. Horsburgh, A. P. Monkman, W. Bras, G. ten Brinke, and O. Ikkala, *Synth. Met.* **121**, 1257 (2001).

<sup>8</sup>A. P. Monkman, M. Halim, I. D. W. Samuel, and L. E. Horsburgh, *J. Chem. Phys.* **109**, 10372 (1998).

<sup>9</sup>M. Knaapila, M. Torkkeli, T. Mäkelä, L. Horsburgh, K. Lindfors, R. Serimaa, M. Kaivola, A. P. Monkman, G. ten Brinke, and O. Ikkala, *Mater. Res. Soc. Symp. Proc.* **660**, JJ5.21.1 (2001).

<sup>10</sup>F. Feller and A. P. Monkman, *Phys. Rev. B* **61**, 13560 (2000).

<sup>11</sup>S. M. Yu, V. P. Conticello, G. Zhang, C. Kayser, M. J. Fournier, T. L. Mason, and D. A. Tirrell, *Nature (London)* **389**, 167 (1997).

<sup>12</sup>O. Dupont, A. M. Jonas, B. Nysten, R. Legras, P. Adriaensens, and J. Gelan, *Macromolecules* **33**, 562 (2000).